European Radiology (2019) 29:6550–6558
https://doi.org/10.1007/s00330-019-06259-9

COMPUTED TOMOGRAPHY

Liver CT perfusion: which is the relevant delay that reduces radiation dose and maintains diagnostic accuracy?

Alessandro Bevilacqua[1,2] · Silvia Malavasi[2,3] · Valérie Vilgrain[4,5]

Received: 30 January 2019 / Revised: 20 April 2019 / Accepted: 30 April 2019 / Published online: 21 May 2019

Abstract

Objectives High radiation dose during CT perfusion (CTp) studies contributes to prevent CTp application in daily clinical practice. This work evaluates the consequences of scan delay on perfusion parameters and provides guidelines to help reducing the radiation dose by choosing the most appropriate delay.

Methods Fifty-nine patients (34 men, 25 women; mean age 68 ± 12) with colorectal cancer, without underlying liver disease, underwent liver CTp, with the acquisition starting simultaneously with iodinated contrast agent injection. Blood flow (BF) and hepatic perfusion index (HPI) were computed on the acquired examinations and compared with those of the same examinations when a variable scan delay (τ) is introduced. Dose length product, CT dose index, and effective dose were also computed on original and delayed examinations.

Results Altogether, three groups of delays ($\tau \leq 4$ s, 5 s $\leq \tau \leq 9$ s, $\tau \geq 10$ s) were identified, yielding increasing radiation dose saving (RDS) (RDS ≤ 9.5%, 11.9% ≤ RDS ≤ 21.4%, RDS ≥ 23.8%) and decreasing perfusion accuracy (high ($\tau \leq 4$ s), medium (5 s $\leq \tau \leq 9$ s), low ($\tau \geq 10$ s)). In particular, single-input and arterial BF and HPI were more insensitive to delay as regards the absolute variations (only 1 ml/min/100 g and 1%, respectively, for $\tau \leq 9$ s), than portal and total BF.

Conclusion Using delays lower than 4 s does not change perfusion accuracy and conveys unnecessary dose to patients. Conversely, starting the acquisition 9 s after contrast agent injection yields a RDS of about 21%, with no significant losses in perfusion accuracy.

Key Points

- *Scan delays lower than 4 s do not alter perfusion accuracy and deliver an unnecessary radiation dose to patients.*
- *Radiation dose delivered to patients can be reduced by 21.4% by introducing a 9-s scan delay, while keeping accurate perfusion values.*
- *Using scan delays higher than 10 s, some perfusion parameters (portal and total BF) were inaccurate.*

Keywords Contrast media · Colorectal neoplasms · Liver diseases · Radiation dosage · Tomography, X-ray computed

Alessandro Bevilacqua and Silvia Malavasi contributed equally to this work.

Electronic supplementary material The online version of this article (https://doi.org/10.1007/s00330-019-06259-9) contains supplementary material, which is available to authorized users.

✉ Valérie Vilgrain
valerie.vilgrain@aphp.fr

[1] DISI (Department of Computer Science and Engineering), University of Bologna, Viale Risorgimento, 2, I-40136 Bologna, Italy

[2] ARCES (Advanced Research Center on Electronic Systems), University of Bologna, Via Toffano 2/2, I-40125 Bologna, Italy

[3] CIG (Interdepartmental Centre "L. Galvani" for integrated studies of Bioinformatics, Biophysics and Biocomplexity), University of Bologna, Via Petroni 26, I-40126 Bologna, Italy

[4] Department of Radiology, Assistance-Publique Hôpitaux de Paris, APHP, HUPNVS, Hôpital Beaujon, 100 bd du Général Leclerc, 92110 Clichy, France

[5] Sorbonne Paris Cité, INSERM CRI, Université Paris Diderot, 75018 Paris, France

Abbreviations

aBF	Arterial blood flow
AD_C	Cohort-oriented absolute differences
AD_P	Patient-oriented absolute differences
BF	Blood flow
$CTDI_{vol}$	Volumetric CT dose index
CTp	CT perfusion
DLP	Dose length product
E_a	Examination acquired
E_τ	Delayed examination
ED	Effective dose
HPI	Hepatic perfusion index
N	Integer number for statistical differences
pBF	Portal blood flow
PD_C	Cohort-oriented percentage differences
PD_P	Patient-oriented percentage differences
p.u.	Perfusion unit
RDS	Radiation dose saved
tBF	Total blood flow
TCCs	Time concentration curves

Introduction

CT perfusion (CTp) is a widely available imaging technique that has aroused lively interest in several clinical applications of the liver [1, 2] such as early tumour detection, characterisation, and prognosis [3–5], fibrosis staging [6, 7], and diagnosis of cirrhosis [8, 9]. However, the high radiation dose delivered to patients during CTp examinations prevents its usage in the daily clinical practice [10, 11], as it adds radiation dose to that of routine examinations [12, 13].

In the last few years, several steps forward have been taken to face this issue, according to two main approaches. The former are applied to standard non-dynamic CT applications like automatic tube current modulation [5], low tube voltage values [14], and iterative reconstruction techniques [15, 16]. The latter are specifically dedicated to dynamic studies and consist in reducing the number of CTp scans acquired. This task is subdivided into three methods: (1) reducing the number of samples by increasing the time period between scans [17]; (2) stopping earlier CTp acquisition during arterial, portal, or equilibrium phases of the tissue time concentration curves (TCCs) [18, 19]; (3) introducing an initial delay between contrast agent administration and CTp acquisition that shortens the unenhanced portion of the TCCs (i.e. baseline). This last method is widely employed in hepatic CTp studies. Indeed, it is very common to find out CTp studies introducing a fixed scan delay between 5 and 10 s [20–23] or a delay chosen through patient-based preliminary scan tests, carried out before perfusion acquisition [24–26].

However, no study exists in the literature discussing how reducing the unenhanced stage ultimately affects perfusion accuracy. Accordingly, the aim of this research was to measure the effects of scan delay on perfusion results computed using the maximum slope that is the most dose-preserving method [27].

Materials and methods

Study population

The present research is an ancillary study of a prospective multicentre trial aiming at assessing the capability of perfusion parameters to predict liver metastasis development in patients with non-metastatic colorectal cancer (PIXEL, PHRC 2007 no. AOM07228). This study had Institutional Review Committee approval and written informed consent provided from all the enrolled patients.

In order to limit the sources of variability, only patients of one centre, the most peopled one, were considered, and 72 patients (39 men, 33 women; mean age 68 ± 13, range 33–89 years) were originally enrolled. According to PIXEL's study protocol, patients free of liver metastases and chronic liver diseases ($n = 70$) were eligible for this study. Patients who received chemotherapy or who underwent cancer colorectal surgery before undergoing liver CTp were not enrolled. Exclusion criteria for this ancillary study were an incorrect field of view preventing perfusion analysis on liver ($n = 3$) and a poor image quality caused by the presence of noise ($n = 3$), artefacts ($n = 3$), or heavy patient motion ($n = 2$). Finally, a total number of 59 patients (34 men, 25 women; mean age 68 ± 12, range 36–89 years) were included in this study (Fig. 1).

Acquisition protocol

All the patients enrolled underwent CTp, carried out using a 64-slice multidetector CT scanner (LightSpeed VCT; GE Healthcare). First, an unenhanced helical CT abdominal scan was performed to localise the portal trunk. Then, an axial CTp acquisition was carried out on the identified region, with patient in the supine feet-first position. During the entire scan sequence, patients were asked to breathe slowly and superficially to limit motion artefacts. Acquisition parameters used for CTp acquisition are reported in Table 1.

Data preparation

Starting from the original CTp examination acquired (E_a), 15 delayed examinations (E_τ, with delay τ varying between 1 and 15 s) were created for each patient, progressively disregarding the first 15 scans to simulate different scan delays (Fig. 2), yielding a total of 944 examinations. To avoid taking advantage from samples unavailable in a protocol designed for the maximum slope, we stopped our virtual acquisitions at 65 s (i.e. considering the first 42 CT scans), roughly corresponding to 5–10 s after the

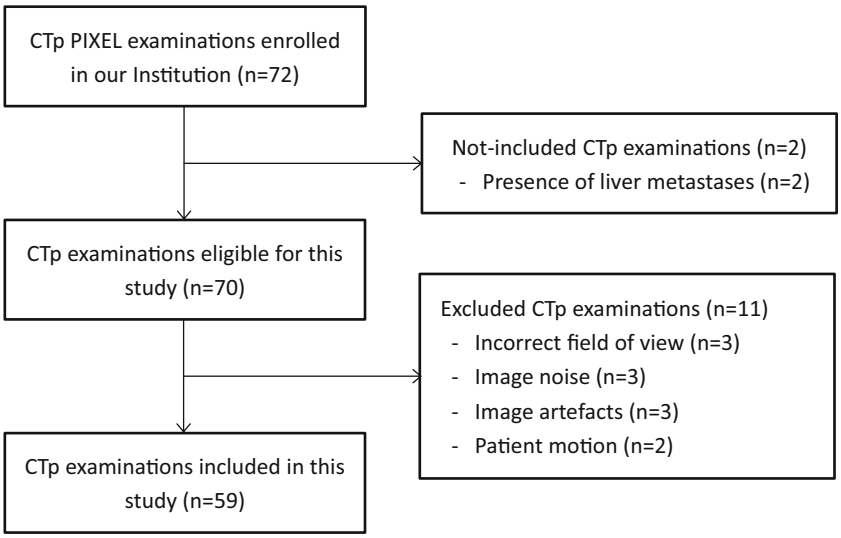

Fig. 1 Flowchart of study enrolment

arterial first pass. As the maximum slope method we used is more sensitive to others to baseline length reduction, we think that our results could be used to other techniques. In fact, differently from the other methods, it exploits only the first portion of the TCC (i.e. the first pass) to compute perfusion parameters, thus suffering more the lack of baseline samples. Finally, ROIs for aorta, portal vein, spleen, and liver were drawn as large as possible on a reference slice of each E_a and used for each E_τ of the same patient as well. An extended explanation is available in "Supplementary Materials".

Data processing and analysis

The 3D motion correction method described in [28] was applied on each E_a to improve data quality. Afterwards, three averaged TCCs were extracted from aorta, portal vein, and spleen ROIs. Instead, voxel-based TCCs drawing out from the tissue ROI were fitted by exploiting a sigmoidal-shaped curve based on the Hill's equation [29]. Finally the maximum slope method, a very popular method for hepatic CTp studies [2], was applied to compute single- and dual-input blood flow (BF, ml/min/100 g) and hepatic perfusion index (HPI, %). In particular, the single-input BF was calculated on each of the 944 examinations, while arterial BF (aBF), portal BF (pBF), total BF (tBF), and HPI were computed in the 768 examinations of the 48 patients where portal vein and spleen were both visible [27, 30]. The perfusion results were displayed using colorimetric maps. Details on perfusion value calculation can be found in "Supplementary Materials".

Table 1 Acquisition protocol parameters. Contrast media protocol and scan parameters related to CTp acquisition

Parameter	Value
Scan width (mm)	40
Slice thickness (mm)	5
Total number of scans	60
Scan delay (s)	0
Cycle time for the first 30 scans (s)	1
Cycle time for the last 30 scans (s)	3
Total acquisition time (s)	120
Tube voltage (kV)	80
Tube current (mA)	100
Exposure (mAs)	100
Contrast media dosage (ml)	40
Iodine concentration (mgI/ml)	350
Contrast media flow (ml/s)	4

Result assessment

For each of the 944 examinations, the median perfusion value of each parameter was calculated and, for each delay τ, resumed through their respective median and interquartile range. Then, in order to quantitatively assess the effects of introducing a non-zero delay τ on CT scans, the perfusion values calculated on the acquired examination E_a and on each delayed examination E_τ were compared. The analysis was carried out at both patient level, to perform a detailed analysis of the effects of delay, and cohort level, to provide averaged resuming indicator values.

First of all, for each patient, the absolute (AD_P) and percentage (PD_P) differences between perfusion values calculated on E_a and each E_τ were computed and, again, summarised through their median and interquartile range. The correlations between each couple of perfusion maps arising from E_a and E_τ of the same patient were calculated by means of Pearson's correlation coefficient (ρ).

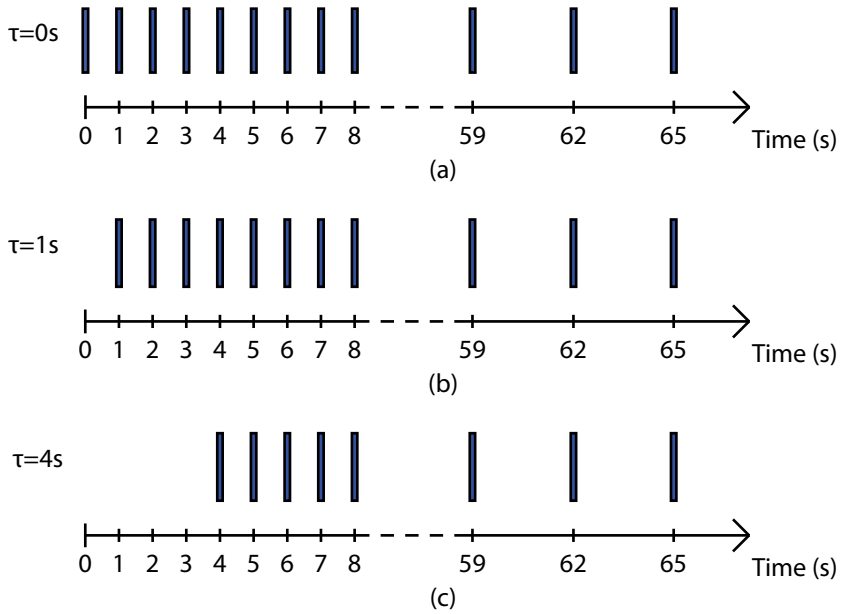

Fig. 2 Blue vertical lines represent CT scans performed to obtain E_a (**a**) and two simulated E_τ achieved by introducing a delay of 1 s (**b**) and 4 s (**c**)

Thereafter, comparisons between perfusion results were carried out at cohort level. In particular, for each patient and perfusion parameter, absolute (AD_C) and percentage (PD_C) differences between the median perfusion values calculated on E_a and E_τ were computed and resumed through median and interquartile range values.

Statistical analysis

In order to favour the clinical translation of results, besides testing whether median absolute and percentage differences between E_a and each E_τ were different from zero, we also tested to what extent they differ, that is, whether they were significantly lower than an integer number N. The one-tail paired Wilcoxon signed-rank test was repeatedly applied to test each AD_P and AD_C on a 20-point scale (i.e. $N = [1 \div 20]$) of perfusion units (p.u., so defined such as to include variations of perfusion parameters having different measurement units, that is "ml/min/100 g" for BF, aBF, pBF, and tBF and "%" for HPI) and each PD_P and PD_C on the percentage scale ($N = [1 \div 100]$). All the statistical tests were performed by using IBM® SPSS® Statistics 23.0 (IBM Corp.), where p value ≤ 0.05 is considered for statistical significance.

Radiation dose analysis

We quantitatively evaluate the benefit for patients in terms of dose reduction through using three widely used radiation dose indicators, i.e. the dose length product (DLP, mGy/mAs), the effective dose (ED, mSv), and the CT dose index ($CTDI_{vol}$, mGy), which also consider the number of CT scans acquired. DLP, ED, and $CTDI_{vol}$ were computed for each examination following the European guidelines [31] (see "Supplementary Materials" for further details), while the radiation dose saved (RDS, in percentage) by introducing the delay τ was calculated for each E_τ according to Eq. 1:

$$\mathrm{RDS} = \frac{j_\tau}{j} \cdot 100 \quad (1)$$

where j_τ is the number of acquisitions saved during τ and j is the number of CT scans considered (here, 42).

Results

Cohort-based analysis

Table 2 reports median and interquartile range of median perfusion values of each examination referred to the whole cohort of patient's obtained for E_a (i.e. with no delay).

Median perfusion AD_C, PD_C, and ρ values obtained for each τ are reported in Table 3. As τ increases, both perfusions AD_c and PD_c increase, while correlation between perfusion values computed on the delayed examinations and the original data acquired decreases. However, global median AD_C are all below 1 (aBF), 2 (single-input BF and HPI), or 3 p.u. (pBF and tBF), independently of delay τ, except for pBF with $\tau = 14$ and $\tau = 15$ s. Instead, global median PD_C are always lower than 10% and, in particular, below 4% (tBF), 6% (BF and pBF), 9% (aBF), and 10% (HPI). Concerning correlation, it was always high ($\rho > 0.90$) except for HPI with $\tau \geq 12$ s.

Patient-based analysis

The voxel-based analysis carried out for each patient shows that median perfusions AD_P and PD_P gradually increase

Table 2 Perfusion values obtained with no scan delay. Perfusion parameters with their median (IQR) values for the acquired examinations are reported, together with the number of patients for which those parameters were computed. *BF* blood flow, *aBF* arterial blood flow, *pBF* portal blood flow, *tBF* total blood flow, *HPI* hepatic perfusion index, *IQR* interquartile range

Perfusion parameters	Perfusion values (median (IQR))	Number of patients
BF (ml/min/100 g)	32.8 (27.4 ÷ 42.3)	59
aBF (ml/min/100 g)	23.0 (16.0 ÷ 30.6)	48
pBF (ml/min/100 g)	92.0 (74.4 ÷ 105.0)	48
tBF (ml/min/100 g)	112.5 (98.5 ÷ 135.6)	48
HPI (%)	21.6 (16.0 ÷ 25.1)	48

according to the scan delay τ (i.e. the baseline shrinks), as expected. Conversely, increasing τ causes a decrease of correlation ρ, between E_a and E_τ, for all perfusion parameters. These trends are depicted in Fig. 3 referring to a sample patient (ID4), showing the median AD_P (a), PD_P (b), and ρ (c) values obtained for each perfusion parameter, as τ varies.

Results of the patient-based statistical analysis are summarised in Fig. 4. Here, for each τ, the highest statistically significant AD_P (Fig. 4a) and PD_P (Fig. 4b) found in at least one patient are reported for each perfusion parameter. For instance, considering $\tau = 7$ s, a maximum AD_P of 2 p.u. has been observed in at least one patient for both tBF and pBF. Instead, AD_P of maximum 1 p.u. have been found for aBF and HPI, while single-input BF has not shown significant AD_P in any patient. In practice, the delays in Fig. 4 can be grouped according to the vertical dashed lines into three different "behaviours" of AD_P and PD_P, whether they keep low and stable ($\tau \leq 4$ s), slowly (5 s $\leq \tau \leq 9$ s), or rapidly increase ($\tau \geq 10$ s).

A practical example of the effects of introducing a scan delay of the second group ($\tau = 9$ s) on perfusion parameters is reported in Fig. 5, which shows the couples of colorimetric maps computed on E_a (a–e) and E_τ ($\tau = 9$ s) (f–j) for patient ID35, the one showing the highest AD_P. For each parameter, perfusion is characterised by practically the same pattern, with excellent correlation ($\rho \geq 0.90$) for BF, aBF, pBF, and tBF. Here, the main differences are the hyper-perfused regions, which are more extended in the "delayed" maps (Fig. 5f–i). Nonetheless, the maximum AD_P for BF, aBF, pBF, and tBF is equal to 1, 1, 3, and 4 ml/min/100 g, respectively. HPI is the perfusion parameter showing the lowest (although quite high) correlation ($\rho = 0.70$). Its colorimetric maps mainly differ in the areas with low perfusion as those calculated with delay

Table 3 Comparison between perfusion results obtained with varying scan delays and no scan delay. Overall median values for AD_C, PD_C, and ρ at different delays τ, referring to BF, aBF, pBF, tBF, and HPI. *BF* blood flow, *aBF* arterial blood flow, *pBF* portal blood flow, *tBF* total blood flow, *HPI* hepatic perfusion index, AD_C cohort-oriented absolute differences, PD_C cohort-oriented percentage differences, ρ Pearson's correlation coefficient, τ delay

Perfusion parameter (median)		τ (s)														
		1	2	3	4	5	6	7	8	9	10	11	12	13	14	15
BF	AD_C (ml/min/100 g)	0.05	0.09	0.15	0.17	0.31	0.37	0.45	0.56	0.65	0.78	0.76	0.90	1.01	1.33	1.75
	PD_C (%)	0.18	0.33	0.49	0.65	0.94	1.17	1.46	1.84	2.09	2.47	2.91	3.45	3.97	4.70	5.49
	ρ	1.00	1.00	0.99	0.99	0.99	0.99	0.98	0.98	0.98	0.97	0.97	0.96	0.94	0.94	0.92
aBF	AD_C (ml/min/100 g)	0.03	0.06	0.07	0.12	0.16	0.20	0.28	0.38	0.36	0.41	0.47	0.57	0.80	0.93	0.99
	PD_C (%)	0.26	0.42	0.68	0.95	1.31	1.59	1.99	2.59	3.01	3.47	4.18	5.07	5.99	7.02	8.54
	ρ	1.00	1.00	0.99	0.99	0.99	0.99	0.98	0.98	0.98	0.97	0.97	0.96	0.95	0.93	0.92
pBF	AD_C (ml/min/100 g)	0.11	0.21	0.34	0.43	0.64	0.94	0.93	1.27	1.39	1.48	1.91	2.21	2.58	3.23	4.03
	PD_C (%)	0.16	0.28	0.44	0.63	0.88	1.09	1.31	1.67	1.94	2.28	2.68	3.17	3.74	4.37	5.25
	ρ	1.00	1.00	0.99	0.99	0.99	0.99	0.98	0.98	0.98	0.97	0.97	0.96	0.95	0.94	0.93
tBF	AD_C(ml/min/100 g)	0.07	0.14	0.20	0.34	0.44	0.54	0.59	0.78	0.92	0.93	1.17	1.27	1.33	1.98	2.16
	PD_C (%)	0.11	0.19	0.30	0.46	0.65	0.80	0.96	1.19	1.40	1.64	1.91	2.24	2.62	3.02	3.50
	ρ	1.00	1.00	1.00	1.00	1.00	0.99	0.99	0.99	0.99	0.98	0.98	0.98	0.97	0.97	0.96
HPI	AD_C (a.u.)	0.02	0.05	0.08	0.09	0.17	0.21	0.28	0.33	0.38	0.40	0.57	0.74	0.86	0.95	1.19
	PD_C (%)	0.27	0.46	0.81	1.04	1.42	1.79	2.28	2.88	3.33	3.90	4.65	5.62	6.64	7.83	9.61
	ρ	1.00	0.99	0.99	0.98	0.98	0.97	0.96	0.95	0.94	0.93	0.91	0.89	0.86	0.85	0.82

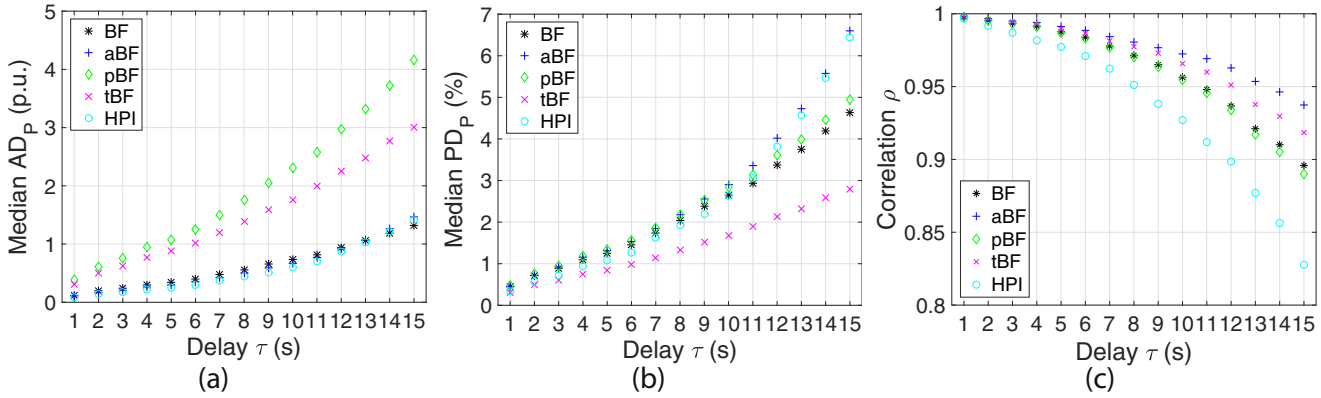

Fig. 3 Median AD_P (**a**), PD_P (**b**), and ρ (**c**) values measured for BF (black asterisk), aBF (blue plus), pBF (green rhomb), tBF (magenta cross), and HPI (cyan circle) maps of a sample patient (ID4), as τ varies

(Fig. 5j) are larger and slightly lower in value than from E_a (Fig. 5e). Accordingly, HPI $AD_P = 0.11$ p.u. is very low (p value $< 10^{-6}$), practically negligible.

Radiation dose

Table 4 shows DLP, ED, and $CTDI_{vol}$ values computed for different scan delays τ together with the RDS as compared with E_a. With the protocol used in this work, each second of delay τ introduced allows saving 2.38% radiation dose.

Discussion

Reducing the number of CT volumes acquired by introducing a scan delay at the beginning of the acquisition, perfusion parameter accuracy decreases as scan delay increases, for single patients and the whole cohort as well. pBF and tBF are the parameters with the highest AD_P. However, as they are the highest perfusion values, they have the lowest PD_P. Conversely, aBF and HPI have the highest PD_P, but their lowest perfusion values yield the lowest AD_P. As far as BF is concerned, it shows the same low AD_P values as aBF and HPI (Fig. 4a) and the same low PD_P value as pBF and tBF (Fig. 4b).

The effects of the delays τ on perfusion parameters are clear at both patient and cohort levels. However, to select the best τ to use in a specific acquisition protocol, we suggest focusing on the patient level, able to emphasise the local heterogeneities [32] and hence more suitable for clinical purposes. In fact, the cohort analysis, the preferred and often the only analysis carried out in many CTp studies, dims the variations observed in single patients. To this purpose, the graphs of Fig. 4 are useful to select the most relevant delay. In the $\tau \leq 4$ s group, no significant $AD_P > 1$ p.u. and $PD_P > 3\%$ were reported. Therefore, by introducing a scan delay of 4 s, it is possible to attain up to RDS = 9.5%, without affecting accuracy. Conversely, if τ is ≥ 10 s, far lower radiations can be administrated to patients (up to RDS = 35.7%), but only BF, aBF, and HPI keep an acceptable accuracy. Finally, if τ is between 5 and 9 s, a significant RDS can be achieved (up to 21.4%), with BF, aBF, and HPI having $AD_P \leq 1$ p.u. and tBF and pBF with $PD_P < 6\%$. All these considerations suggest considering a delay of 9 s.

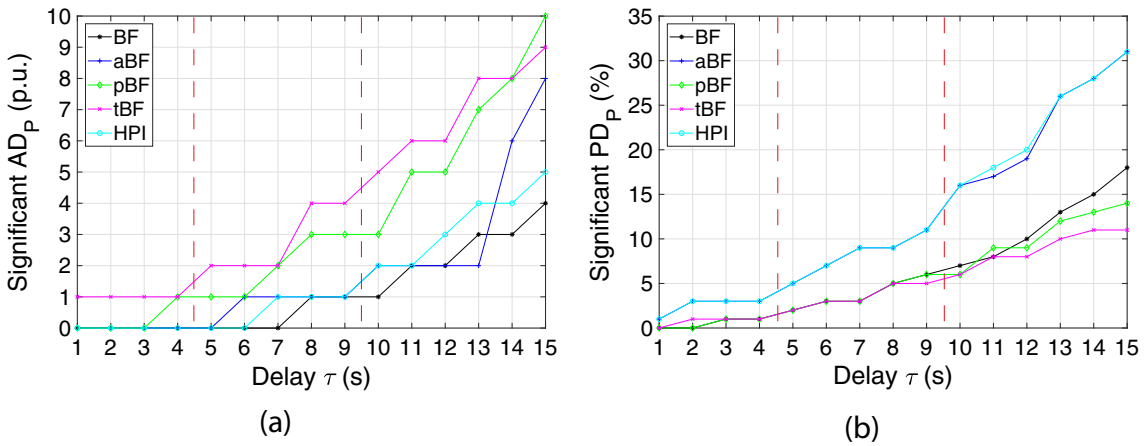

Fig. 4 For each delay τ, the highest statistically significant median AD_P (**a**) and PD_P (**b**) found in at least one patient are reported for BF (black asterisk), aBF (blue plus), pBF (green rhomb), tBF (magenta cross), and HPI (cyan circle). The graphs can be split into three main regions according to the red broken dashed lines. Each region is characterised by different degrees of perfusion results accuracy and RDS

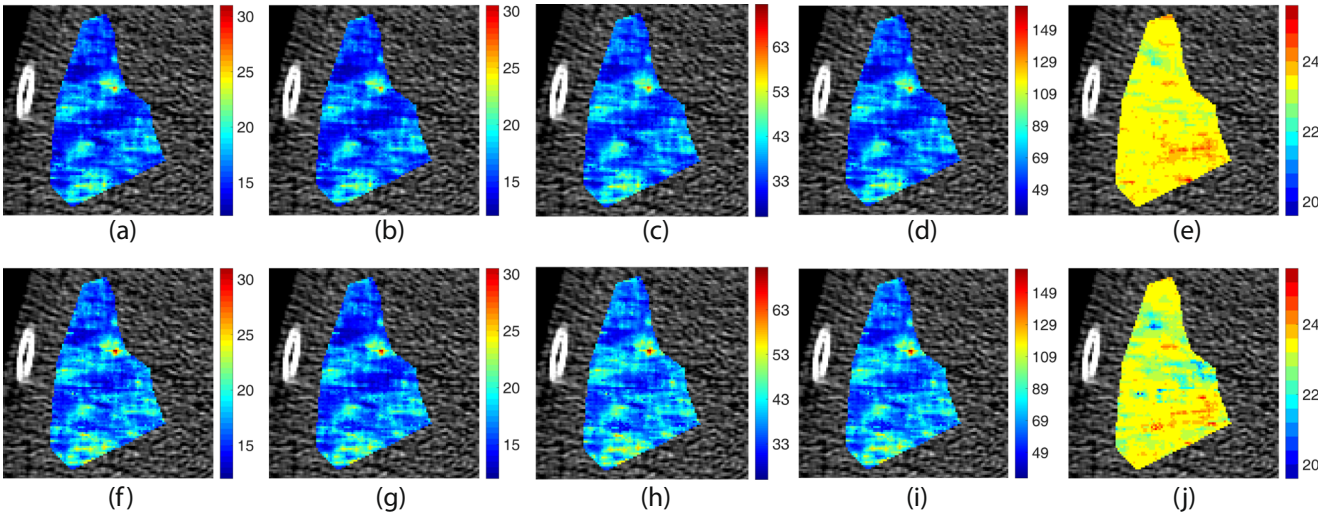

Fig. 5 Colorimetric maps of BF (**a**, **f**), aBF (**b**, **g**), pBF (**c**, **h**), tBF (**d**, **i**), and HPI (**e**, **j**) computed for patient ID35 on its E_a (**a**–**e**) and its E_τ (**f**–**j**), obtained with a $\tau = 9$ s

Our results are in good agreement with other studies [17, 18]: by diminishing the number of acquired volumes, it is possible to save radiation dose, but at the expense of higher perfusion variations. In particular, one study [18] analysing the effects of stopping the acquisition earlier highlights that perfusion parameters are better estimated if a longer acquisition is used. Indeed, the authors considered the single-input BF values were within a satisfactory confidence level only for acquisitions lasting at least 160 s. This is achieved by avoiding the last three samples and allows RDS = 5% (with ED decreasing from 28 to 26.6 mSv), yielding an $AD_C = 1$ ml/min/100 g. Instead, by using our approach and delaying the acquisition by $\tau = 9$ s, it is possible to achieve RDS = 21.4% (with ED decreasing from 10.3 to 8.1 mSv), with single-input BF $AD_C < 1$ ml/min/100 g. With a different approach, one study tested the effect on single-input BF (computed with maximum slope) of increasing time between consecutive scans at different exposures [17]. The authors found that by increasing the time interval between consecutive scans, from 1 to 2 s or 4 s, it was possible to achieve RDS up to 50% and 75%, respectively. By acquiring only one volume every 4 s at 100 mAs (the same exposure as in our study), $CTDI_{vol}$ decreases from 1.76 to 0.44 mGy, but introducing a very high BF $AD_C = 5.7$ ml/min/100 g. With 400 mAs, sampling one volume every 2 s and 4 s yields AD_C of 0.5 ml/min/100 g and 4.1 ml/min/100 g, but with $CTDI_{vol}$ of 3.54 mGy and 1.77 mGy, respectively. Instead, by using our approach and delaying the acquisition of 9 s, BF AD_C is similar, with $CTDI_{vol}$ of only 1.35 mGy.

There are mainly three limitations to this study. First, the results could be different if perfusion parameters were computed by different methods than maximum slope. However, the chosen model is the most sensitive to baseline shortening since it exploits only the first TCCs' portion [14]; therefore, we expect that perfusion parameters computed with other methods would show lower variations, or at the most similar, as compared with maximum slope. Second, the absolute outcome could vary when using different scan parameters or contrast agent administration rate, although the percentage of RDS remains unchanged. Finally, these results were not tested on patients with chronic liver disease and cannot necessarily apply to this population.

In conclusion, reducing acquisition scan duration by delaying the beginning of CTp acquisition allows significant radiation dose saving, while maintaining an acceptable accuracy. Using delay lower than 4 s conveys unnecessary radiation dose. With a delay of 9 s, 21.4% of radiation dose can be saved with an acceptable reduction in accuracy.

Table 4 Radiation dose for different scan delays. DLP, ED, $CTDI_{vol}$, and RDS for increasing values of the scan delay τ. Columns 0–4, 5–9, and 10–15 refer to the same three regions highlighted in Fig. 4a. *DLP* dose length product, *ED* effective dose, *$CTDI_{vol}$* volumetric CT dose index, *RDS* radiation dose saved, τ delay

Radiation dose	τ (s)															
	0	1	2	3	4	5	6	7	8	9	10	11	12	13	14	15
DLP (mGy cm)	685.4	669.1	652.8	636.5	620.2	603.8	587.5	571.2	554.9	538.6	522.2	505.9	489.6	473.3	457.0	440.6
ED (mSv)	10.3	10.0	9.8	9.5	9.3	9.1	8.8	8.6	8.3	8.1	7.8	7.6	7.3	7.1	6.9	6.6
CTDIvol (mGy)	1.71	1.67	1.63	1.59	1.55	1.51	1.47	1.43	1.39	1.35	1.31	1.26	1.22	1.18	1.14	1.10
RDS (%)	0.0	2.4	4.8	7.1	9.5	11.9	14.3	16.7	19.0	21.4	23.8	26.2	28.6	31.0	33.3	35.7

Funding This study has received funding by a grant from the Programme Hospitalier de Recherche Clinique - PHRC 2007 no. AOM07228, France, and sponsored by Assistance-Publique Hôpitaux de Paris (APHP).

Compliance with ethical standards

Guarantor The scientific guarantor of this publication is Prof. Valérie Vilgrain.

Conflict of interest The authors of this manuscript declare no relationships with any companies whose products or services may be related to the subject matter of the article.

Statistics and biometry Alessandro Bevilacqua, MS, PhD, kindly provided statistical advice for this manuscript and is one of the authors of this manuscript.

Informed consent Written informed consent was waived by the Institutional Review Board.

Ethical approval Institutional Review Board approval was obtained.

Methodology
- Retrospective
- Diagnostic or prognostic study
- Performed at one institution

References

1. Oğul H, Kantarcı M, Genç B et al (2014) Perfusion CT imaging of the liver: review of clinical applications. Diagn Interv Radiol 20: 379–389
2. Kartalis N, Brehmer K, Loizou L (2017) Multi-detector CT: liver protocol and recent developments. Eur J Radiol 97:101–109
3. Kim SH, Kamaya A, Willmann JK (2014) CT perfusion of the liver: principles and applications in oncology. Radiology 272:322–344
4. Ippolito D, Querques G, Okolicsanyi S et al (2018) Dynamic contrast enhanced perfusion CT imaging: a diagnostic biomarker tool for survival prediction of tumour response to antiangiogenetic treatment in patients with advanced HCC lesions. Eur J Radiol 106:62–68
5. Nakamura Y, Kawaoka T, Higaki T et al (2018) Hepatocellular carcinoma treated with sorafenib: arterial tumor perfusion in dynamic contrast-enhanced CT as early imaging biomarkers for survival. Eur J Radiol 98:41–49
6. Horowitz JM, Venkatesh SK, Ehman RL et al (2017) Evaluation of hepatic fibrosis: a review from the society of abdominal radiology disease focus panel. Abdom Radiol (NY) 42:2037–2053
7. Thaiss WM, Sannwald L, Kloth C et al (2018) Quantification of hemodynamic changes in chronic liver disease: correlation of perfusion-CT data with histopathologic staging of fibrosis. Acad Radiol. https://doi.org/10.1016/j.acra.2018.11.009
8. De Robertis R, D'Onofrio M, Demozzi E, Crosara S, Canestrini S, Pozzi Mucelli R (2014) Noninvasive diagnosis of cirrhosis: a review of different imaging modalities. World J Gastroenterol 20: 7231–7241
9. Fischer MA, Marquez HP, Gordic S et al (2017) Arterio-portal shunts in the cirrhotic liver: perfusion computed tomography for distinction of arterialized pseudolesions from hepatocellular carcinoma. Eur Radiol 27:1074–1080
10. Marquez HP, Karalli A, Haubenreisser H et al (2017) Computed tomography perfusion imaging for monitoring transarterial chemoembolization of hepatocellular carcinoma. Eur J Radiol 91: 160–167
11. Fischer MA, Kartalis N, Grigoriadis A et al (2015) Perfusion computed tomography for detection of hepatocellular carcinoma in patients with liver cirrhosis. Eur Radiol 25:3123–3132
12. Ippolito D, Querques G, Okolicsanyi S, Franzesi CT, Strazzabosco M, Sironi S (2017) Diagnostic value of dynamic contrast-enhanced CT with perfusion imaging in the quantitative assessment of tumor response to sorafenib in patients with advanced hepatocellular carcinoma: a feasibility study. Eur J Radiol 90:34–41
13. Perisinakis K, Tzedakis A, Pouli S, Spanakis K, Hatzidakis A, Damilakis J (2019) Comparison of patient dose from routine multi-phase and dynamic liver perfusion CT studies taking into account the effect of iodinated contrast administration. Eur J Radiol 110:39–44
14. Marquez HP, Puippe G, Mathew RP, Alkadhi H, Pfammatter T, Fischer MA (2017) CT perfusion for early response evaluation of radiofrequency ablation of focal liver lesions: first experience. Cardiovasc Intervent Radiol 40:90–98
15. Kalra MK, Sodickson AD, Mayo-Smith WW (2015) CT radiation: key concepts for gentle and wise use. Radiographics 35:1706–1721
16. Lell MM, Wildberger JE, Alkadhi H, Damilakis J, Kachelriess M (2015) Evolution in computed tomography: the battle for speed and dose. Invest Radiol 50:629–644
17. Ramirez-Giraldo JC, Thompson SM, Krishnamurthi G et al (2013) Evaluation of strategies to reduce radiation dose in perfusion CT imaging using a reproducible biologic phantom. AJR Am J Roentgenol 200:W621–W627
18. Ng CS, Hobbs BP, Chandler AG et al (2013) Metastases to the liver from neuroendocrine tumors: effect of duration of scan acquisition on CT perfusion values. Radiology 269:758–767
19. Ng CS, Chandler AG, Yao JC et al (2014) Effect of pre-enhancement set-point on CT perfusion values in normal liver and metastases to the liver from neuroendocrine tumors. J Comput Assist Tomogr 38:526–534
20. Lee DH, Lee JM, Klotz E, Han JK (2016) Multiphasic dynamic computed tomography evaluation of liver tissue perfusion characteristics using the dual maximum slope model in patients with cirrhosis and hepatocellular carcinoma: a feasibility study. Invest Radiol 51:430–434
21. Fischer MA, Brehmer K, Svensson A, Aspelin P, Brismar TB (2016) Renal versus splenic maximum slope based perfusion CT modelling in patients with portal-hypertension. Eur Radiol 26: 4030–4036
22. Kako Y, Yamakado K, Jomoto W et al (2017) Changes in liver perfusion and function before and after percutaneous occlusion of spontaneous portosystemic shunt. Jpn J Radiol 35:366–372
23. Jiang T, Kambadakone A, Kulkarni NM, Zhu AX, Sahani DV (2012) Monitoring response to antiangiogenic treatment and predicting outcomes in advanced hepatocellular carcinoma using image biomarkers, CT perfusion, tumor density, and tumor size (RECIST). Invest Radiol 47:11–17
24. Tamandl D, Waneck F, Sieghart W et al (2017) Early response evaluation using CT-perfusion one day after transarterial chemoembolization for HCC predicts treatment response and long-term disease control. Eur J Radiol 90:73–80
25. Gill AB, Hilliard NJ, Hilliard ST, Graves MJ, Lomas DJ, Shaw A (2017) A semi-automatic method for the extraction of the portal venous input function in quantitative dynamic contrast-enhanced CT of the liver. Br J Radiol. https://doi.org/10.1259/bjr.20160875
26. Mulé S, Pigneur F, Quelever R et al (2018) Can dual-energy CT replace perfusion CT for the functional evaluation of advanced hepatocellular carcinoma? Eur Radiol 28:1977–1985
27. Miles KA, Hayball MP, Dixon AK (1993) Functional images of hepatic perfusion obtained with dynamic CT. Radiology 188:405–411

28. Bevilacqua A, Barone D, Malavasi S, Gavelli G (2014) Quantitative assessment of effects of motion compensation for liver and lung tumors in CT perfusion. Acad Radiol 21:1416–1426
29. Gibaldi A, Barone D, Gavelli G, Malavasi S, Bevilacqua A (2015) Effects of guided random sampling of TCCs on blood flow values in CT perfusion studies of lung tumors. Acad Radiol 22:58–69
30. Blomley MJ, Coulden R, Dawson P et al (1995) Liver perfusion studied with ultrafast CT. J Comput Assist Tomogr 19:424–433
31. Menzel H, Schibilla H, Teunen D (2000) European guidelines on quality criteria for computed tomography. European Commission Publication, Luxembourg No. EUR 16262 EN. Available via https://publications.europa.eu/en/publication-detail/-/publication/d229c9e1-a967-49de-b169-59ee68605f1a. Accessed 10 Mar 2019
32. Malavasi S, Barone D, Gavelli G, Bevilacqua A (2017) Multislice analysis of blood flow values in CT perfusion studies of lung cancer. Biomed Res Int 2017:3236893